DOI: 10.1002/asia.200700131

# Elucidating the Coordination Chemistry and Mechanism of Biological Nitrogen Fixation

Ian Dance*[a]

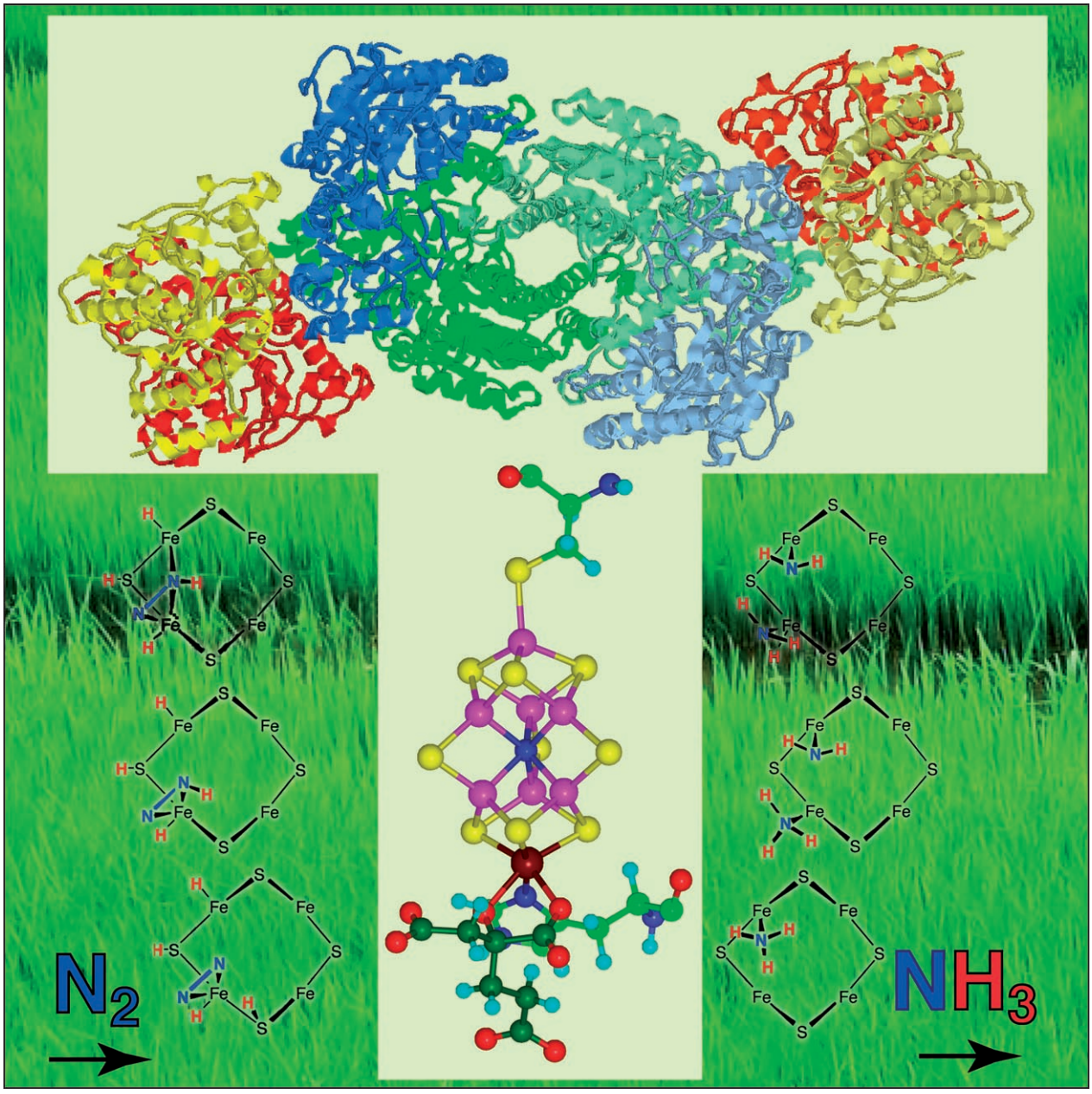

**Abstract:** How does the enzyme nitrogenase reduce the inert molecule $N_2$ to $NH_3$ under ambient conditions that are so different from the energy-expensive conditions of the best industrial practices? This review focuses on recent theoretical investigations of the catalytic site, the iron–molybdenum cofactor FeMo-co, and the way in which it is hydrogenated by protons and electrons and then binds $N_2$. Density functional calculations provide reaction profiles and activation energies for possible mechanistic steps. This establishes a conceptual framework and the principles for the coordination chemistry of FeMo-co that are essential to the chemical mechanism of catalysis. The model advanced herein explains relevant experimental data.

**Keywords:** allosterism · coordination chemistry · density functional calculations · nitrogen fixation · reaction mechanisms

## 1. Introduction

Dinitrogen ($N_2$) is a very unreactive molecule, yet all of life on earth ultimately depends on the $N_2 \rightarrow NH_3$ stage of the global nitrogen cycle. Approximately half of the total fixation of atmospheric dinitrogen occurs biologically, as effected by nitrogenase enzymes in bacteria that are symbiotic mainly with leguminous plants. The remainder takes place in the production of industrial fertilizers with the Haber–Bosch technology.[1] There is a stark contrast between the conditions of enzymatic fixation—subatmospheric pressure and ambient temperature—and the high temperatures and pressures of the Haber–Bosch process, which uses more than 1% of human energy consumption.[1] Apart from economic and environmental considerations in the nitrogenase versus Haber–Bosch dichotomy,[1,2] there is also a fundamental chemical curiosity: how does nitrogenase reduce $N_2$ under such mild conditions?

Much is known about the structure of the enzyme proteins and the biochemical mechanism.[3–8] There are two metalloproteins, the MoFe protein and the Fe protein. Figure 1 shows half of the pseudodimeric MoFe protein docked with the Fe protein. The iron–molybdenum cofactor (FeMo-co), at which catalysis occurs, and the P cluster, which mediates electron transfer, are inside the MoFe protein. The Fe protein contains two ATP/ADP molecules and one $Fe_4S_4$ cluster, which are also involved in electron transfer. The key biochemical cycle (known as the Fe protein cycle) involves three processes: 1) association of the reduced Fe protein (including two MgATP complexes) and the MoFe protein, 2) hydrolysis of MgATP, which enables transfer of one electron to the MoFe protein (via $Fe_4S_4$ and the P cluster), and 3) dissociation of the two protein molecules, exchange of ATP back into the Fe protein, and re-reduction of the Fe protein.

This biochemical cycle delivers electrons to the P cluster (which undergoes some structural changes that involve the surrounding protein[10]) and then (by an enigmatic pathway[6]) to FeMo-co. At this point, the questions about chem-

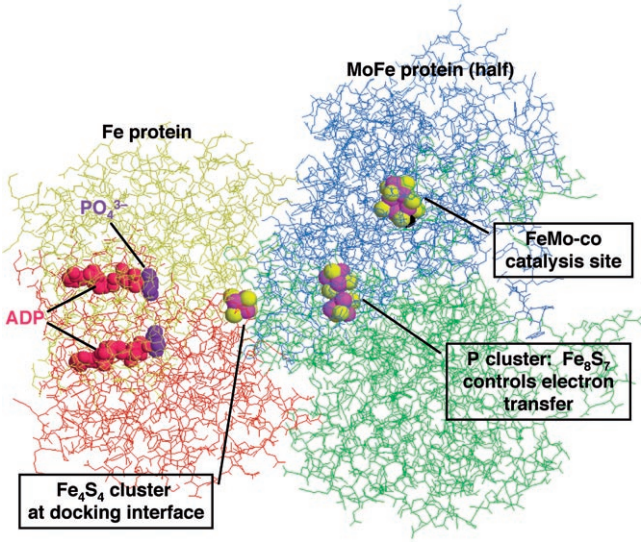


Figure 1. The principal components of nitrogenase (*Azotobacter vinelandii*). The two chains of the Fe protein are in yellow and red; two of the four chains of the pseudodimeric MoFe protein are in blue and green. Taken from the crystal structure (Protein Database 1N2C) of the docked proteins stabilized with $AlF_4^-$ in place of $PO_4^{3-}$.[9]

[a] Prof. I. Dance
School of Chemistry
University of New South Wales
Sydney 2052 (Australia)
E-mail: I.Dance@unsw.edu.au

  

ical catalysis arise. How do the substrate $N_2$ and the protons reach FeMo-co? How does $N_2$ bind to FeMo-co? What is the sequence of multiple steps in which electrons and protons are progressively added to $N_2$, and via what intermediates, until $NH_3$ is formed? How does $NH_3$ leave? Over the decades of experimental research into these questions, there have been three main areas of progress. In the 1980s, Thorneley and Lowe made detailed kinetic measurements of nitrogenase activity, from which they developed a mechanistic scheme that involves a sequence of reduced (hydrogenated) levels of FeMo-co denoted $E_1H_1$, $E_2H_2$, $E_3H_3$, $E_4H_4$, and concluded that productive involvement of $N_2$ occurs at the $E_3H_3$ and $E_4H_4$ levels.[11] In 1992, the unexpected and unprecedented structure of FeMo-co was revealed,[12] with further refinement in 2002.[13] Recent investigations of the effects of modification of surrounding residues revealed the location of catalytic activity on the surface of FeMo-co.[14]

As shown in Figure 2, FeMo-co is an $Fe_7MoS_9$ metal-sulfide cluster that contains a small central atom of unproven elemental identity, but most probably nitrogen ($N^c$ in Figure 2a).[15–18] This cluster is akin to a fused pair of cubes. There are three μ-S (double) bridges around the central belt and six $\mu_3$-S (triple) bridges at the ends. The Fe1 end is ligated by cysteine-275,[19] whereas the Mo atom at the other end is ligated by histidine-442 and chelated by the hydroxy and carboxy donors of a homocitrate cofactor ((*R*)-2-hydroxy-1,2,4-butanetricarboxylic acid), which is essential for activity.[20] In this resting state, Mo is six-coordinate, and each of the Fe atoms is four-coordinate. The side chains of two amino acids, histidine-195 and arginine-96, form hydrogen bonds with μ-S atoms S2B and S5A, respectively, in the resting state (Figure 2b), and modification of His195 in particular affects nitrogenase activity. The side chain of glutamine-191, in the same α-helix as His195, hydrogen-bonds to a dangling carboxylate of homocitrate and is also sensitive to mutation-induced reactivity changes. Modification of residue 70 was most informative: if the alkane side chain is increased in size (valine to isoleucine), reactivity with $N_2$ or the alternative substrate $C_2H_2$ is diminished, whereas if the side-chain volume is decreased (valine to alanine), nitrogenase is able to reduce the larger substrates propargyl alcohol ($CH_2$=$CHCH_2OH$) and hydrazine.[21–25] Modification of Gly69 was also informative.[26] The conclusion from the full

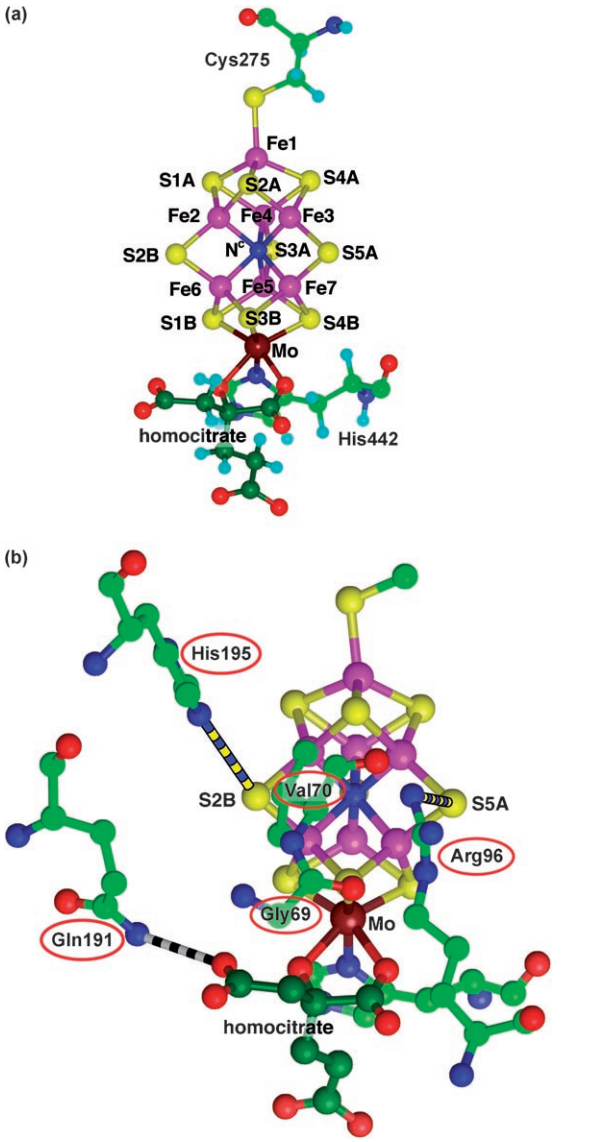


Figure 2. a) Detailed structure and atom labels for resting-state FeMo-co (crystal structure 1M1N), linked to the MoFe protein via Cys275 and His442 and with homocitrate (C atoms in dark green) chelating Mo. The elemental identity of the central atom $N^c$ is unproven. b) Influential residues surrounding FeMo-co. Hydrogen bonds are shown striped. The side chain of Val70 is located directly over Fe2 and Fe6.

***Ian Dance*** *studied with Hans Freeman in Sydney, Jack Lewis in Manchester, and Richard Holm at M.I.T. He is Emeritus Professor of Chemistry at the University of New South Wales and a Fellow of the Australian Academy of Science. His research interests include structural chemistry and intermolecular interactions, metal chalcogenides and thiolates, and applications of density functional theory in inorganic and bioinorganic chemistry.*

results of these experiments is that $N_2$ and $C_2H_2$ bind to one or both of the Fe atoms closest to these side chains, that is, to Fe2 and/or Fe6.[14]

All the evidence indicates that the face of FeMo-co is constituted by the atoms Fe2, S2B, Fe6, S3B, Fe7, and S5A; Fe3 and S2A make up the reactive catalytic site.[14,21,27,28]

Further experimental progress in revealing aspects of the nitrogenase mechanism was confounded by several fundamental difficulties, apart from the general complexity of the reactions and the sensitivity of the proteins to oxygen. One impediment is the lack of an ESR signal during turnover of the wild-type enzyme, and the consequent inability to observe intermediates during turnover directly. A second is the

  

fact that $N_2$ does not bind in the resting state of the enzyme. A third is the unavoidability of the proton as an alternative substrate (reduction to $H_2$), and therefore difficulty in interrupting normal turnover to characterize intermediates. A review in 2000 opened with the statement "Rationality notwithstanding, anyone studying nitrogenase should be excused for occasionally wondering whether a Faustian bargain might be required to establish the mechanism of dinitrogen by this enzyme."[29] Since then, the progress that has been made in the detection of intermediates has involved mutant proteins and freeze-quenching.[24,25,30–32]

## 2. Theory

### 2.1. Role of Theory

When experimental investigations into chemical mechanisms become difficult and frustrating, the importance of theoretical methods is enhanced. The conventional role of theory is in postexperimental interpretation, but in problems such as the nitrogenase mechanism, theoretical methods can make primary contributions. In particular, it is possible to use density functional theory (DFT) to calculate with good accuracy the electronic structure and energy of FeMo-co, which then permits simulation of the reactivity of the catalytic site and its reactants, intermediates, and products. This investigative methodology and its advantages are outlined below.

The calculations focus on the potential-energy surfaces (i.e., geometry–energy relationships) for the most-stable electronic and spin states of postulated species. The goal is to identify favorable reaction intermediates and reaction pathways and to characterize the individual steps of possible reaction sequences from reactant to product. This is possible because the DFT methodology described below, which relies on powerful computers, is sufficiently efficient to permit investigation of hundreds of species and reaction steps that involve FeMo-co with bound small molecules.

### 2.2. Procedures for Theoretical Investigation

The engine of this research is DFT calculation of molecular electronic structure and energy, which includes calculation of the gradient of the energy–geometry surface and optimization of geometrical structure by minimization of energy. These calculations require selection of the functional in the Hamiltonian that relates energy to electron density and selection of the basis set of atomic orbitals. I used the standard BLYP functional and numerical basis sets in my calculations. The principal advantage of numerical basis sets over more-conventional analytical basis sets such as Gaussian functions is their markedly increased computational speed without loss of accuracy.[33,34] All my calculations were performed with the DMol3 program.[34,35]

It is essential that the accuracy of this methodology be assessed; this was done with reference to relevant experimental data on FeMo-co, related metal-sulfide clusters, and coordination complexes that contain $N_2$, $H_2$, and H ligands.[36–39] The validation calculations involve both geometric and reaction-energy data. This DMol DFT methodology yields bonding that is very slightly weaker than the true value, with bond-length discrepancies of less than 0.05 Å.

As expected for a sulfide cluster that contains eight transition metals, the electronic structure of FeMo-co is complex, and there are about 20 molecular orbitals within 1 eV of the highest-occupied (HOMO) and lowest-unoccupied (LUMO) molecular orbitals: the HOMO–LUMO gap is usually about 0.4 eV. Alternative electronic and spin states of FeMo-co are sometimes close in energy to the ground state and, therefore, need to be monitored and controlled during calculation of reaction profiles. These alternative electronic and spin states have different distributions of electronic spin density on the metal atoms.[40–42]

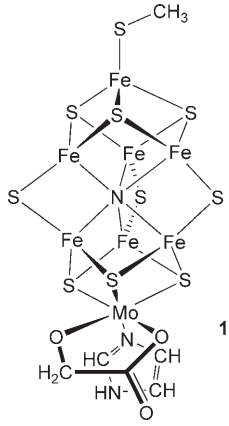

1

The model used to calculate FeMo-co is **1**, in which His442 is truncated to imidazole, Cys275 is truncated to $SCH_3$, and homocitrate is truncated to glycolate ($^-OCH_2COO^-$); this retains the native coordination of all the metal atoms. My calculations were all-electron (i.e., no simplification of core orbitals), spin-unrestricted, and had no imposed symmetry. The resting molecular-oxidation state was defined by the net charge of −3 for **1**, as previously established.[43]

When investigating reaction mechanisms, it is important to know the relative energies of the intermediates and transition states (TSs). Conventional methods for computing a TS have some difficulties when applied to FeMo-co and its derivatives, owing to its complex electronic and vibrational structure. Therefore, I developed a simple and reliable method to locate the lowest-energy saddle point with zero gradient between reactant and product, based on small-step small-range energy minimizations of structures that cycle iteratively from one side of the barrier to the other.[44] This iterative cycle automatically optimizes all other geometrical variables and, with diminishing excursions along the reaction coordinate, converges the gradient to zero. Care was taken to ensure that the reactant, transition, and product states lie on one electronic surface by calculating the complete profile from reactant to TS to product.

The strategy is to explore all conceivable structures with substrates and intermediates bound to FeMo-co, thus developing an appreciation of the geometry–energy surfaces for potentially relevant species and an understanding of the general principles of the coordination chemistry of FeMo-co. With this information, reaction steps are postulated and their energy profiles calculated. Then, with cognizance of all pertinent experimental data, the most-probable reaction sequences and intermediates are developed and assessed.

Clearly, computational modeling of the metalloenzyme mechanism should include the surrounding protein. Com-

  

plete DFT calculation is impractical, and various approximate treatments can be used.[45] I tested a continuum solvation approximation (COSMO), in which the charge distribution of ligated FeMo-co polarizes a virtual surrounding dielectric medium and generates electrostatic energies, which are included in the calculation. For the systems tested, it was estimated that the errors incurred by neglect of the electronic influences of the surrounding protein were less than 0.05 Å in geometry;[44] hence, most calculations ignored the surrounding protein. Although this is reasonable for broad explorations of plausible mechanisms, calculations that specifically include the chemical behavior of the surrounding protein will eventually be needed for promotable mechanisms. I previously reported calculations that assess the geometric compatibility of ligated FeMo-co models with the surrounding protein.[28,39,44]

Four other research groups reported DFT investigations of the full FeMo-co structure. Two of these (Nørskov and Blöchl and their co-workers) used a different calculational setup, with infinite repetition of the chemical molecular model that was sufficiently separated to simulate isolated molecules, and with plane-wave basis sets and frozen core orbitals.[46,47] Blöchl and co-workers used molecular dynamics to optimize the geometries, with additional constraints to determine transition states.[47] Lovell and co-workers calculated individual FeMo-co molecules, with the surrounding protein taken into account, and focused on the physical properties of FeMo-co rather than its reactions.[45] Cao et al. used **1** as model of FeMo-co, as well as DMol methodology, and focused on Mo as the reactive site.[48,49]

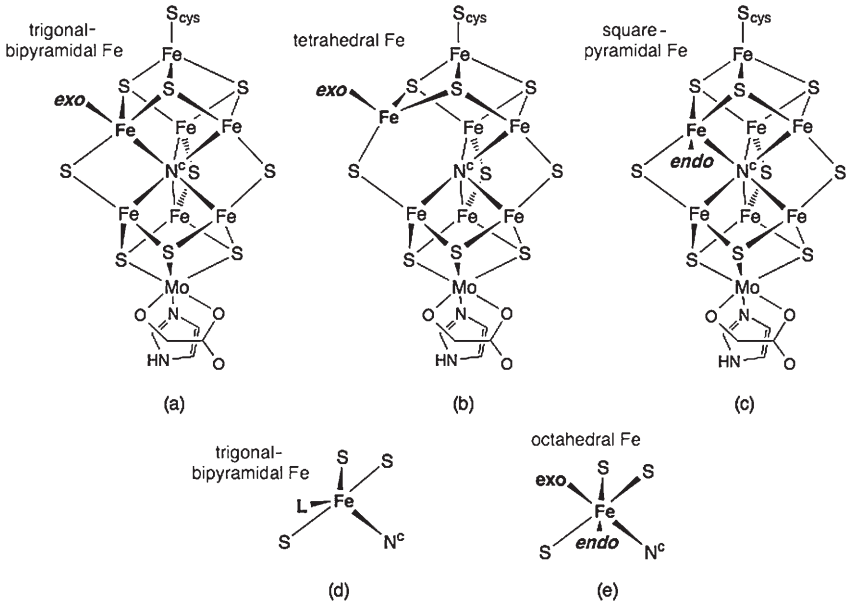


Scheme 1. Coordination possibilities of FeMo-co. Each can occur at any of the six central Fe atoms.

## 3. Coordination Chemistry

### 3.1. Coordination Chemistry of FeMo-co

The calculated partial charges on FeMo-co and its derivatives generally range from +0.25 to +0.4 on the Fe atoms, +0.8 on Mo, −0.3 to −0.6 on S, and −0.3 to −0.4 on $N^c$, and I regard FeMo-co accordingly as being maintained by polar covalent bonding. In general, FeMo-co has some plasticity, and from the small energy changes associated with variation of metal–metal distances it is evident that metal–metal bonding is weak. Each of the six central Fe atoms of resting-state FeMo-co has approximate trigonal-pyramidal coordination ($S_3FeN^c$). Additional ligation can occur *trans* to Fe–$N^c$, in the coordination position labeled *exo* (Scheme 1). This *exo* ligation can occur with only a small extension (typically to 2.2 Å) of the Fe–$N^c$ bond, which leads to regular trigonal-bipyramidal coordination at Fe (Scheme 1a); alternatively, *exo* ligation can cause marked outwards displacement of Fe to break the Fe–$N^c$ bond and elongate it to about 3 Å, such that Fe has a regular tetrahedral coordination (Scheme 1b). For some *exo* ligands, the short and long Fe–$N^c$ isomers both occupy local energy minima with similar energies. There is another coordination position around each of the central Fe atoms, labeled *endo* (Scheme 1c). For this to occur, the doubly bridging S atom bound to Fe needs to fold back a little so that the S–Fe–S angles change from approximately trigonal to approximately orthogonal, and the *endo* ligand L completes the approximately square pyramidal $LS_3Fe–N^c$ coordination (Scheme 1c).

The distinction between the *exo* and *endo* coordination positions at Fe involves only angular changes, and there is an arc of coordination positions between the *exo* and *endo* extremes. If the ligand L is partway along this arc, there is approximately trigonal-bipyramidal coordination at Fe (Scheme 1d). However, this is uncommon: L usually occupies the *exo* or *endo* positions. It is also possible for two ligands to coordinate Fe at the *exo* and *endo* positions, thus yielding octahedral coordination (Scheme 1e).

All the coordination possibilities illustrated in Scheme 1 are involved in the intermediates in the calculated mechanisms of $N_2$ reduction. The central Fe atoms clearly can have variable coordination number (4, 5, 6) and flexible coordination stereochemistry, which are the attributes required for catalytic metal centers.

  

CHEMISTRY
AN ASIAN JOURNAL

### 3.2. Coordinative Allosterism: Role of the Central Atom

An interesting and significant property of FeMo-co arises from the elongation and weakening of the Fe–$N^c$ bond. It was observed in many calculations that whereas one Fe–$N^c$ bond can elongate substantially to about 3 Å and be effectively nonexistent, the severance of two Fe–$N^c$ bonds does not occur. Let us consider Fe2 and Fe6 (the two most-likely participants in catalysis): when one is about 3 Å from $N^c$, the length of the other Fe–$N^c$ bond was found to be constrained to less than 2.5 Å. The lengths/strengths of the two Fe–$N^c$ bonds are thus correlated. This correlation between the positions of two Fe atoms is not caused by the S atom that bridges them, but is due to $N^c$. If the central atom is removed, the $(\mu\text{-}S)_3Fe_6$ region of ligated FeMo-co can undergo extreme distortion: it is clear that one role of the multiply bridging central atom is to control the flexibility of FeMo-co, which cannot be done by the doubly bridging S atoms. Another role of the central atom is to transmit bonding effects between Fe atoms.

The explanation involves the bonding capacities of Fe and $N^c$. Six-coordinate $N^c$ in unligated FeMo-co is abnormal and overbonded, and therefore can readily sever a bond to Fe provided that there is sufficient energy compensation in the other bonds to Fe. However, severance of both Fe2–$N^c$ and Fe6–$N^c$ leaves $N^c$ under- and irregularly coordinated, and is therefore resisted. The strength of the L–Fe bond inversely affects that of the *trans* Fe–$N^c$ bond, and as L could be $N_2$, $H_2$, H, HN(NH), $H_2N(NH_2)$, or $NH_3$ (as well as inhibitors such as CO) in the catalytic mechanism, considerable variation in both L–Fe and Fe–$N^c$ bond strengths is to be expected and is found in the calculations. These effects are transmitted through $N^c$ between Fe atoms. In the sequence $L_A$–Fe2–$N^c$–Fe6–$L_B$ (Scheme 2), the nature and strength of the $L_A$–Fe2 bond affect those of the Fe6–$L_B$ bond, and vice versa. In this way, allosteric relationships develop between these coordination sites.

By analogy with the general occurrence of allosterism in enzymes and proteins (e.g., hemoglobin[50]), this phenomenon in FeMo-co is named coordinative allosterism.[39] The effect is illustrated in Scheme 2 for *exo* coordination of Fe, but *endo* and/or *exo* coordination of Fe are observed to participate in allosteric relationships that can be pronounced or quite subtle.

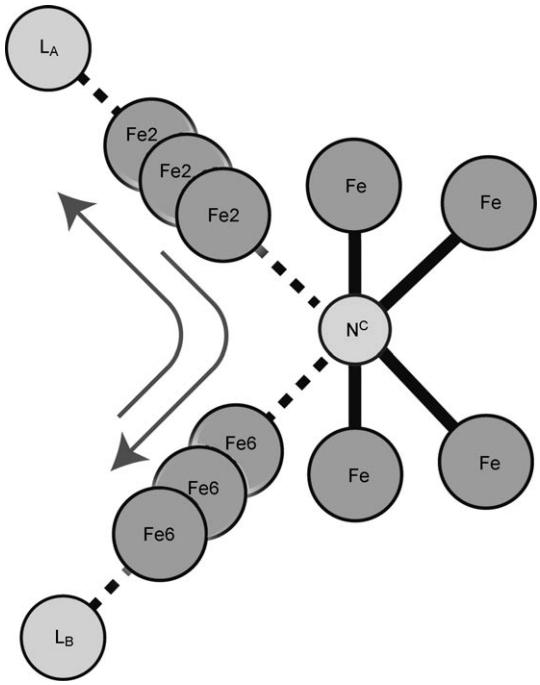


Scheme 2. The concept of coordinative allosterism, in which the $L_A$–Fe2 and $L_B$–Fe6 bonds mutually influence each other via $N^c$. $L_A$ and $L_B$ can be the substrates, intermediates, inhibitors, and products of the catalytic cycle.

## 4. Hydrogen Supply

The reduction of one $N_2$ molecule requires six $H^+$ ions and six electrons, and in nitrogenase is invariably accompanied by further electronation (incorporation of an electron) of $H^+$ to generate $H_2$. A fundamental issue is the supply of electrons and protons to FeMo-co and then $N_2$ during its reduction. The pathway for electron transfer from the P cluster to FeMo-co is unknown and has received little speculative comment. For the proton supply, it is sometimes assumed that the required protons will be transferred to electronated $N_2$ on FeMo-co from the surrounding amino acids or water molecules. However, examination of the protein crystal structures showed that the protein surrounding the likely catalytic sites on the reactive face of FeMo-co is both hydrophobic and anhydrous. The side chains of His195 and Arg96 (hydrogen-bonded to S2B and S5A, respectively, in the resting-state protein; Figure 2b) may appear to be suitable proton donors, but there is no evident pathway for proton replenishment to these side chains, and it is difficult to see how they could be cycled to provide sufficient protons. A more-likely role for these hydrogen bonds is modulation of FeMo-co behavior.[51]

There are two water molecules in the vicinity of FeMo-co. One, HOH208, is located 5.3 Å from S2A, 4.1 Å from Fe3, and 3.4 Å from S5A, and is hydrogen-bonded in a closed set of water molecules. The second water molecule of interest is HOH679, which is located 4.0 Å from S3B, and is the terminus of two extended water hydrogen-bonding networks,[39] one of which is shown in part in Figure 3. The chain of 15 water molecules that culminates in HOH679 also involves hydrogen bonds to three of the O atoms of homocitrate, which is consistent with the strict requirement for homocitrate in nitrogenase.[20] The mechanistic importance of HOH679 is emphasized by its conserved occurrence and location in all the high-resolution crystal structures.[39] It was proposed that the chain of water molecules shown in Figure 3 is the one that repetitively shuttles protons to S3B during catalysis. A detailed hypothesis was provided[39] for the carriage of protons from HOH50 to HOH679 and on to S3B by using adjoining amino acids and three O atoms of

  

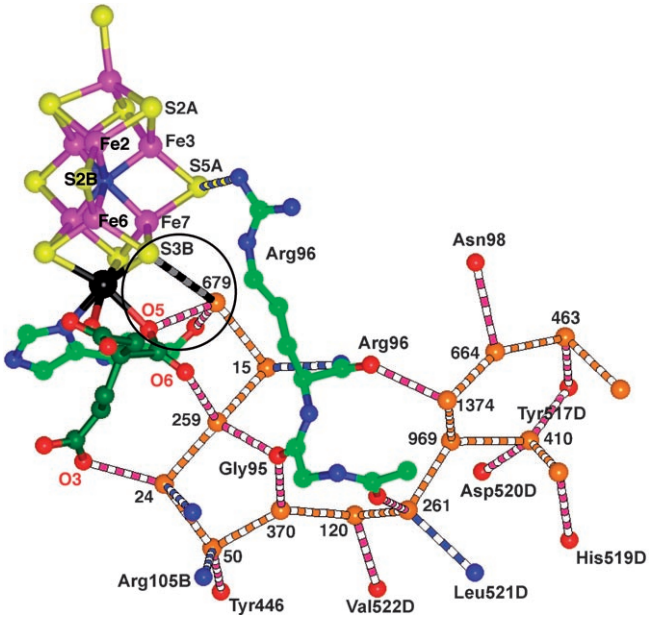


Figure 3. The putative proton-supply chain, culminating in water molecule 679. The proximity of HOH679 to S3B (black and grey stripes), O5 of homocitrate, and the carbonyl O of His442 is emphasized by the black circle. Water molecules are in orange, other atoms involved in the chain are in red (O) and blue (N), homocitrate O atoms are labeled in red, hydrogen bonds are shown striped. The residues labeled D are in the δ chain of the MoFe protein.

homocitrate as proton buffers. Other authors also recognized this putative proton-supply chain.[42,51,52]

It was calculated that electron transfer to FeMo-co concentrates increased negative charge on its S atoms, thus increasing their basicity. Therefore, an electron transferred onto FeMo-co will promote transfer of $H^+$ from HOH679 to S3B (S3B moves towards HOH679 during this process). From S3B, an H atom can migrate to other Fe and S atoms of FeMo-co, and possibly transfer to bound substrate molecules and intermediates, thus allowing S3B to receive a subsequent proton. Scheme 3 outlines the processes proposed to generate the reducing H atoms (which have partial charges between +0.1 and −0.1) on FeMo-co.

There are numerous ways in which one or more H atoms can be bound to FeMo-co, including S–H, *endo*- and *exo*-

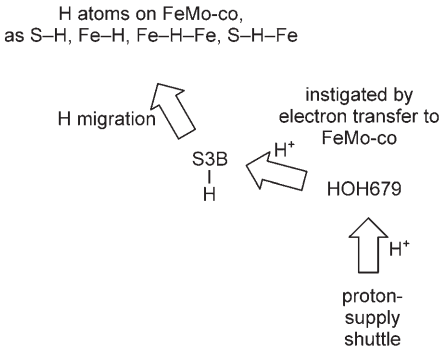


Scheme 3. Pathway for repeated hydrogenation of FeMo-co.

Fe–H, *endo*- and *exo*-Fe–$H_2$, and Fe–H–Fe and S–H–Fe bridges. These, as well as the calculated reaction profiles for the movement of H atoms between S and Fe, for the generation of Fe–$H_2$, for the association and dissociation of Fe–$H_2$ at various hydrogenation levels, and for H/$H_2$ exchange, have been reported.[39,53] This detailed description of the hydrogen chemistry of FeMo-co connects significantly with the earlier Thorneley–Lowe mechanistic schemes and the $E_1H_1$, $E_2H_2$, $E_3H_3$, and $E_4H_4$ reduced states of FeMo-co. The DFT calculations have now mapped the structural possibilities for these $E_nH_n$ species.

## 5. Structural Mechanistic Model

At this point, a structural mechanistic model was developed for the catalytic hydrogenation reactivity at FeMo-co:[53]

1) After electron transfer to FeMo-co, H atoms are generated by fast proton supply to S3B, which then migrate through several pathways to various locations on the FeMo-co face (Figure 4a). The activation energies for H migration were calculated to be 5–15 kcal mol$^{-1}$.
2) Each of the $E_nH_n$ levels of the Thorneley–Lowe mechanism is potentially a sequence of substructures with different distributions of the H atoms, which develop at FeMo-co during and independent of the cycle of association/dissociation of the MoFe and Fe proteins (the Fe protein cycle).
3) Substrates, particularly $N_2$ and $C_2H_2$ ($C_2H_2$ is not a natural substrate, but is experimentally and mechanistically significant), can bind at Fe6 and Fe2. Details of the dynamics of the coordination of $N_2$ and $C_2H_2$ depend on the number and distribution of H atoms on FeMo-co,

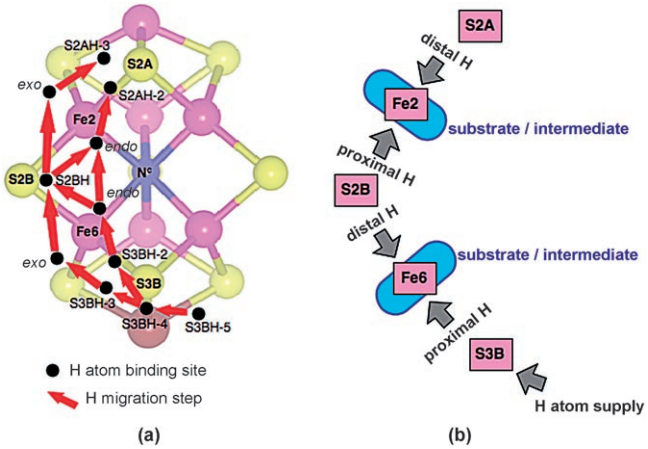


Figure 4. a) Relevant H-atom binding sites and migration pathways on FeMo-co. The different configurations of S3B–H and S2A–H are labeled, as are the *endo* and *exo* positions at Fe6 and Fe2. b) Generalized model for the provision of H atoms to substrates or intermediates bound to Fe2 or Fe6 (blue ovals). The squares represent the possible locations of H atoms in the reduced states of FeMo-co. The proximal and distal directions for the addition of H atoms to substrates/intermediates are marked.

  

and this provides the conceptual framework for the observation that $N_2$ is productively bound only at the $E_3H_3$ and $E_4H_4$ levels, whereas $C_2H_2$ is productively bound at the $E_1H_1$ and $E_2H_2$ levels.[11,54]

4) The reduction of the substrates and their intermediates on the path to the products occurs by transfer of H atoms from the S and Fe atoms of FeMo-co.
5) The migration of H atoms is unidirectional, or vectorial, because there is only one source, S3B–H. The coordination of substrates and intermediates at Fe6 or Fe2 blocks the migration of H atoms past these sites. Therefore, proximal and distal directions for H addition to substrates/intermediates are created (Figure 4b). At the stage of substrate binding, there can be pre-positioned H atoms in either or both of the proximal and distal positions, but additional H atoms required for transfer to the intermediates can only be provided from the proximal direction. This is significant for the reduction of $N_2$, which requires six H atoms.
6) There is a general synergy in which the location of H atoms influences the dynamics of substrate binding, and substrate binding influences H-atom migration.

This general structural mechanistic model was developed further to provide a unified explanation for much of the experimental data, which include a) the two-site reactivity of $C_2H_2$ and the differentiation of the high- and low-affinity sites (due to different preparatory H migration), b) the differing mutual inhibitions of $N_2$ and $C_2H_2$ in wild-type proteins, c) the modified reactivity of the α-Gly69→α-Ser69 mutant with $N_2$ and $C_2H_2$, and d) the stereoselective hydrogenation of $C_2D_2$ and its loss in some mutant proteins (Scheme 4).[53]

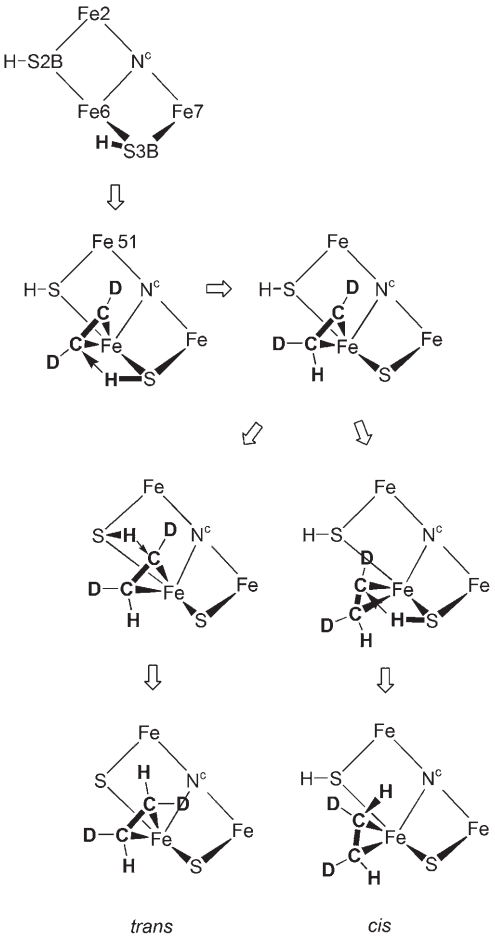


Scheme 4. Mechanism proposed for stereospecific hydrogenation of $C_2D_2$ at Fe6.

## 6. Binding of $N_2$ to FeMo-co

The question of how $N_2$ binds to FeMo-co is fundamental. In the absence of sufficiently relevant or informative experimental data ($N_2$ binding to FeMo-co appears to have been detected[25,31] but not characterized), there have been several calculations. $N_2$ can bond to the Fe atoms of FeMo-co with $\eta^1$ (end-on) or $\eta^2$ (side-on) geometries and in the *exo* or *endo* positions. The degree and type of hydrogenation of FeMo-co (with H atoms and possibly an $H_2$ molecule) influence the details of $N_2$ binding. The most comprehensive investigation described 94 different structures (as local energy minima) with varying degrees of hydrogenation and $N_2$ bound to either Fe6 or Fe2.[44] The stabilities of 57 of these structures were assessed by calculation of the reaction profiles and activation energies for the association and dissociation of $N_2$. Barriers to association of $N_2$ are dependent mainly on the locations of hydrogenation and $N_2$ coordination, whereas dissociation barriers are related primarily to whether $N_2$ is $\eta^1$- or $\eta^2$-coordinated, and secondarily on the location of hydrogenation. No energy minima were found for $N_2$ molecules bridging two, three, or four of the atoms of the Fe2–Fe3–Fe6–Fe7 face of FeMo-co. Some examples of structures with $N_2$ bound to hydrogenated FeMo-co are shown in Figure 5, together with their profiles for association and dissociation of $N_2$.

Hinemann and Nørskov suggested the *exo*-$\eta^1$ coordination of $N_2$ at Fe, with three H atoms on the three μ-S atoms, as the most-stable structure with bound $N_2$.[46] The calculations of Kästner, Blöchl, and co-workers led them to two structures (Scheme 5) in which the Fe7–S5A–Fe3 bridge is broken and replaced by terminal Fe3–SH: $N_2$ first binds in an $\eta^1$ fashion to Fe7, then bridges between Fe7 and Fe3.[42,47,55] These structures are less consistent with the general coordination chemistry of metal-sulfide clusters,[56] in which ($\mu_3$-S)–M bonds are more-readily disrupted than (μ-S)–M bonds. Structure 1-4H-a in Figure 5 is an example of typical FeMo-co behavior, with an elongated Fe6–S3B bond when S3B is hydrogenated. There are difficulties in translocating the coordination at Fe3 and Fe7 shown in Scheme 5 to Fe2 and Fe6 (the most-probable reaction sites) due to interference with the surrounding protein.[44]

What then can be concluded about how $N_2$ binds to FeMo-co? The many possibilities alluded to above were fur-

  

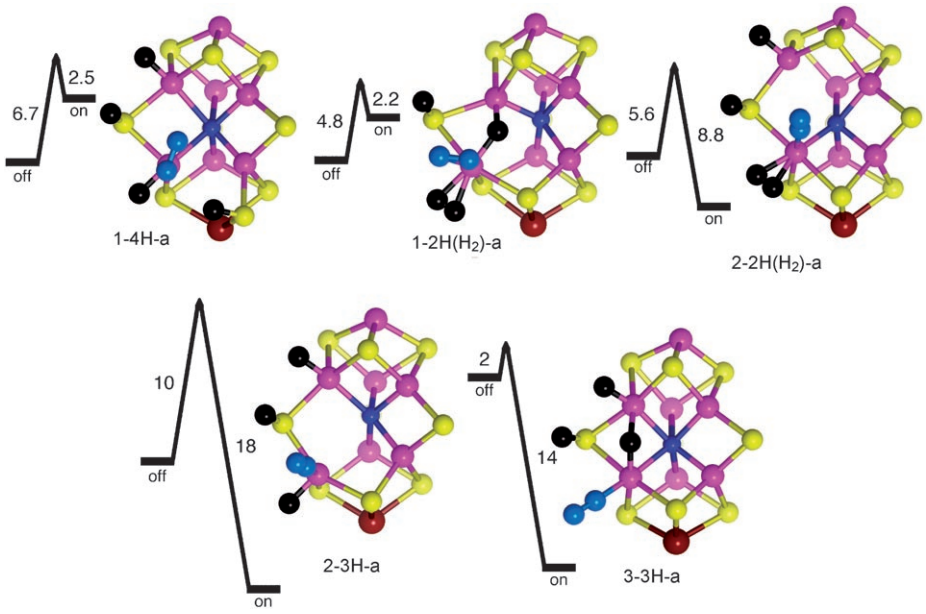


Figure 5. Five examples of structures with $N_2$ (blue) bound to Fe6 of hydrogenated (H atoms in black) FeMo-co. The additional coordination of Fe1 (top) and Mo (bottom), included in the calculations, is not shown. In the reaction profiles to the left of each structure, the associated and dissociated states are labeled on and off, respectively, and the activation energies (kcal mol$^{-1}$) are marked. Structure identifiers are those of the original paper.[44]

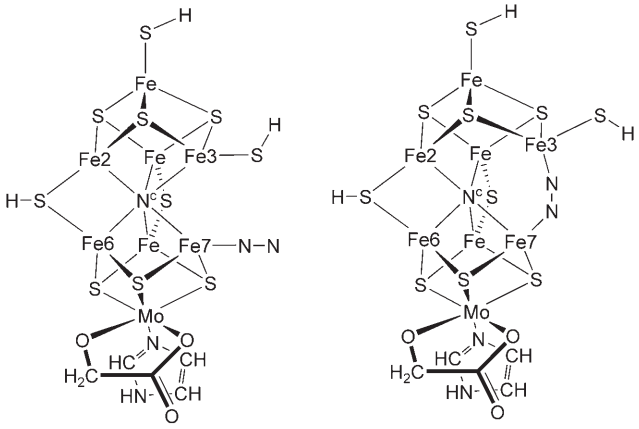


Scheme 5. The structures proposed by Kästner, Blöchl, and co-workers for $N_2$ bound to doubly hydrogenated FeMo-co.

ther evaluated in terms of their interactions with the surrounding protein and their compatibility with the experimental reactivity data from key mutant proteins, which led to the suggestion that *endo*-$\eta^1$-$N_2$ coordination at Fe6 is most-probable.[44] However, any conclusion is tempered by the requirement that the energy barrier for the next step, the transfer of H to bound $N_2$, be surmountable, and that there be feasible subsequent steps in the mechanism.

## 7. Mechanisms for Conversion of $N_2$ into $NH_3$

The stage for the molecular dance in which $N_2$ becomes $NH_3$ is now set, with knowledge of the structures of FeMo-co and the surrounding protein. The prospective molecular dancers are known: they are the hydrogenated forms of FeMo-co and the species with bound $N_2$. Now we can explore the choreography of this molecular dance,[57] and calculations of the profiles for these mechanistic steps are in progress. It appears that mechanisms that involve H transfer to *endo*-$\eta^1$-bound $N_2$ have higher activation barriers than those that involve H transfer to *endo*-$\eta^2$-$N_2$. The key objective at this time is to determine the most-favorable overall combination of steps for prehydrogenation of FeMo-co, binding of $N_2$, sequential H transfer to bound $N_2$, breaking of the N–N bond, all the way to the formation and dissociation of $NH_3$. In tests so far, there is no significant difference between reaction profiles for $N^c$ or $C^c$ as the central atom of FeMo-co, and it appears that the unproven identity of the central atom is not an important issue in the elucidation of the mechanism.

Kästner and Blöchl very recently described a mechanism for the conversion of $N_2$ into $NH_3$, starting from the structures in Scheme 5 and operating at Fe3 and Fe7 with a severed Fe7–S5A bond and terminal Fe7–SH coordination.[55] They assumed that protons are supplied by the surrounding residues modeled with $NH_4^+$ as a nonspecific proton source.

## 8. Understanding the FeMo-co Mechanism

Recent experimental results from Seefeldt, Dean, Hoffman, and co-workers[14,21] have been invaluable for locating the site of catalytic chemical action on the face of FeMo-co. Experimental characterization of intermediates in the mechanism, though, is more difficult: instead of the previously mentioned Faustian bargain, it may be more appropriate in this journal to contemplate Brajendra Nath Seal and his epic poem "Quest Eternal".[58] In the meantime, DFT calculations are advancing specific hypotheses for the key mechanistic intermediates and steps, and are developing a unified conceptual framework for understanding and refining the mechanism. The principal tenets of this framework are: a) the reduction of substrates by direct hydrogenation,

  

CHEMISTRY
AN ASIAN JOURNAL

which involves transfer of H atoms from atoms bound to the same face of FeMo-co, rather than directly from the surrounding residues to the substrate; b) the ability of the proton chain terminating at HOH679 to generate H atoms on S3B (probably synchronous with electronation of FeMo-co); c) the vectorial migration of H atoms from S3B to Fe6, S2B, Fe2, and S2A; d) the blockage of H transfer by bound substrates and intermediates, thus causing a differentiation of proximal (replenishable) and distal (nonreplenishable) H-atom transfers to substrates and intermediates; e) substrate binding influenced and controlled by the degree and location of prior hydrogenation of FeMo-co.

The justification for this conceptual framework is that it enables the explanation of much of the biochemical data on the reactivity of $N_2$ and $C_2H_2$ with wild-type and modified nitrogenase.[53] Furthermore, tenets a), b), c), and e) provide the basis for assigning structures to the $E_nH_n$ intermediate states of the Thorneley–Lowe kinetic schemes.

## 9. Interpreting FeMo-co

The picture that is developing from these DFT calculations also suggests rationalization of the structure and function of FeMo-co and its components, as well as of the surrounding protein. I offer these interpretations: 1) the central Fe atoms (particularly Fe6 and Fe2), with trigonal-pyramidal coordination in the resting state, each provide one or two adaptable coordination sites for the reactants and intermediates; 2) the six-coordinate Mo atom provides a crucial anchoring role, connecting with the surrounding protein (via His442), linking homocitrate (which maintains the proton supply chain) with S3B as the H entry point, and orientating these features in relation to Fe6 as a principal coordination site; 3) the central atom (either $N^c$ or $C^c$) prevents extreme distortion of FeMo-co and connects the Fe atoms where coordinative reaction occurs, thus transmitting coordinative information between them and enabling coordinative allosterism; 4) the full structure of FeMo-co, as two cubanoid $M_4S_3$ entities linked by four atoms ($(\mu\text{-}S)_3+N^c$), is required to provide geometrical integrity for the reactive $N^cFe_4(\mu\text{-}S)_2(\mu_3\text{-}S)_2$ face, which would otherwise be mechanically unstable; 5) the protein surrounding the Fe6 and Fe2 catalytic sites is hydrophobic, which is consistent with both the character of the incoming physiological substrate $N_2$ and the control of the hydrogenation reactions from the catalytic site rather than the surrounding amino acids; 6) the homocitrate ligand fosters the water pool in the $NH_3$ product exit domain; 7) amino acid His195, which is able to hydrogen-bond with S2B or S2B–H, has a role in connecting and regulating the hydrogenation state of FeMo-co with movements of surrounding protein.

## 10. Conclusions

DFT calculations are making good progress in the understanding of the chemistry of the natural fixation of dinitrogen and the properties of the catalytic site.

## Acknowledgements

This research is supported by The Australian Partnership for Advanced Computing and the University of New South Wales.

[1] V. Smil, *Enriching the Earth: Fritz Haber, Carl Bosch, and the Transformation of World Food Production*, MIT Press, Cambridge, MA, **2001**.
[2] J. Sarukhan, A. Whyte, *Millennum Ecosystem Assessment, 2005: Ecosystems and Human Well-Being: Synthesis*, Island Press, Washington, D.C., **2005**.
[3] B. K. Burgess, D. J. Lowe, *Chem. Rev.* **1996**, *96*, 2983–3011.
[4] B. E. Smith, *Adv. Inorg. Chem.* **1999**, *47*, 159–218.
[5] J. Christiansen, D. R. Dean, L. C. Seefeldt, *Annu. Rev. Plant Physiol. Plant Mol. Biol.* **2001**, *52*, 269–295.
[6] R. Y. Igarashi, L. C. Seefeldt, *Crit. Rev. Biochem. Mol. Biol.* **2003**, 38, 351–384.
[7] D. C. Rees, F. A. Tezcan, C. A. Haynes, M. Y. Walton, S. Andrade, O. Einsle, J. A. Howard, *Philos. Trans. R. Soc. London Ser. A* **2005**, *363*, 971–984.
[8] J. W. Peters, R. K. Szilagyi, *Curr. Opin. Chem. Biol.* **2006**, *10*, 101–108.
[9] H. Schindelin, C. Kisker, J. L. Schlessman, J. B. Howard, D. C. Rees, *Nature* **1997**, *387*, 370–376.
[10] J. W. Peters, M. H. B. Stowell, S. M. Soltis, M. G. Finnegan, M. K. Johnson, D. C. Rees, *Biochemistry* **1997**, *36*, 1181–1187.
[11] R. N. F. Thorneley, D. J. Lowe in *Molybdenum Enzymes* (Ed.: T. G. Spiro), Wiley Interscience, New York, **1985**, pp. 221–284.
[12] J. Kim, D. C. Rees, *Nature* **1992**, *360*, 553–560.
[13] O. Einsle, F. A. Tezcan, S. L. A. Andrade, B. Schmid, M. Yoshida, J. B. Howard, D. C. Rees, *Science* **2002**, *297*, 1696–1700.
[14] P. C. Dos Santos, R. Y. Igarashi, H.-I. Lee, B. M. Hoffman, L. C. Seefeldt, D. R. Dean, *Acc. Chem. Res.* **2005**, *38*, 208–214.
[15] I. Dance, *Chem. Commun.* **2003**, 324–325.
[16] B. Hinnemann, J. K. Nørskov, *J. Am. Chem. Soc.* **2003**, *125*, 1466–1467.
[17] T. Lovell, T. Liu, D. A. Case, L. Noodleman, *J. Am. Chem. Soc.* **2003**, *125*, 8377–8383.
[18] V. Vrajmasu, E. Munck, E. L. Bominaar, *Inorg. Chem.* **2003**, *42*, 5974–5988.
[19] Throughout this article, atom and amino acid labels are those of structure 1M1N in the Protein Structural Database.
[20] J. Imperial, T. R. Hoover, M. S. Madden, P. W. Ludden, V. K. Shah, *Biochemistry* **1989**, *28*, 7796–7799.
[21] B. M. Barney, R. Y. Igarashi, P. C. Dos Santos, D. R. Dean, L. C. Seefeldt, *J. Biol. Chem.* **2004**, *279*, 53621–53624.
[22] R. Y. Igarashi, P. C. Dos Santos, W. G. Niehaus, I. G. Dance, D. R. Dean, L. C. Seefeldt, *J. Biol. Chem.* **2004**, *279*, 34770–34775.
[23] H.-I. Lee, R. Y. Igarashi, M. Laryukhin, P. E. Doan, P. C. Dos Santos, D. R. Dean, L. C. Seefeldt, B. M. Hoffman, *J. Am. Chem. Soc.* **2004**, *126*, 9563–9569.
[24] B. M. Barney, M. Laryukhin, R. Y. Igarashi, H.-I. Lee, P. C. Dos Santos, T.-C. Yang, B. M. Hoffman, D. R. Dean, L. C. Seefeldt, *Biochemistry* **2005**, *44*, 8030–8037.
[25] B. M. Barney, H.-I. Lee, P. C. Dos Santos, B. M. Hoffman, D. R. Dean, L. C. Seefeldt, *Dalton Trans.* **2006**, 2277–2284.
[26] J. Christiansen, V. L. Cash, L. C. Seefeldt, D. R. Dean, *J. Biol. Chem.* **2000**, *275*, 11459–11464.

  

[27] L. C. Seefeldt, I. G. Dance, D. R. Dean, *Biochemistry* **2004**, *43*, 1401–1409.
[28] I. Dance, *J. Am. Chem. Soc.* **2004**, *126*, 11852–11863.
[29] D. C. Rees, J. B. Howard, *Curr. Opin. Chem. Biol.* **2000**, *4*, 559–566.
[30] R. Y. Igarashi, M. Laryukhin, P. C. Dos Santos, H.-I. Lee, D. R. Dean, L. C. Seefeldt, B. M. Hoffman, *J. Am. Chem. Soc.* **2005**, *127*, 6231–6241.
[31] B. M. Barney, T.-C. Yang, R. Y. Igarashi, P. C. Dos Santos, M. Laryukhin, H.-I. Lee, B. M. Hoffman, D. R. Dean, L. C. Seefeldt, *J. Am. Chem. Soc.* **2005**, *127*, 14960–14961.
[32] B. M. Barney, D. Lukoyanov, T.-C. Yang, D. R. Dean, B. M. Hoffman, L. C. Seefeldt, *Proc. Natl. Acad. Sci. USA* **2006**, *103*, 17113–17118.
[33] B. Delley, *J. Chem. Phys.* **1990**, *92*, 508–517.
[34] B. Delley, *J. Chem. Phys.* **2000**, *113*, 7756–7764.
[35] B. Delley in *Modern Density Functional Theory: A Tool for Chemistry, Vol. 2* (Eds.: J. M. Seminario, P. Politzer), Elsevier, Amsterdam, **1995**, pp. 221–254.
[36] I. G. Dance in *Transition Metal Sulfur Chemistry: Biological and Industrial Significance*, *Vol. 653* (Eds.: E. I. Stiefel, K. Matsumoto), American Chemical Society, Washington, D.C., **1996**, pp. 135–152.
[37] C. Bianchini, D. Masi, M. Peruzzini, M. Casarin, C. Maccato, G. A. Rizzi, *Inorg. Chem.* **1997**, *36*, 1061–1069.
[38] I. Dance, *Chem. Commun.* **1998**, 523–530.
[39] I. Dance, *J. Am. Chem. Soc.* **2005**, *127*, 10925–10942.
[40] T. Lovell, J. Li, T. Liu, D. A. Case, L. Noodleman, *J. Am. Chem. Soc.* **2001**, *123*, 12392–12410.
[41] T. Lovell, J. Li, D. A. Case, L. Noodleman, *J. Biol. Inorg. Chem.* **2002**, *7*, 735–749.
[42] J. Schimpl, H. M. Petrilli, P. E. Blöchl, *J. Am. Chem. Soc.* **2003**, *125*, 15772–15778.
[43] I. Dance, *Inorg. Chem.* **2006**, *45*, 5084–5091.
[44] I. Dance, *J. Am. Chem. Soc.* **2007**, *129*, 1076–1088.
[45] L. Noodleman, T. Lovell, W.-G. Han, J. Li, F. Himo, *Chem. Rev.* **2004**, *104*, 459–508.
[46] B. Hinnemann, J. K. Nørskov, *J. Am. Chem. Soc.* **2004**, *126*, 3920–3927.
[47] J. Kästner, S. Hemmen, P. E. Blöchl, *J. Chem. Phys.* **2005**, *123*, 074306.
[48] Z. Cao, Z. Zhou, H. Wan, Q. Zhang, *Int. J. Quantum Chem.* **2005**, *103*, 344–353.
[49] Z. X. Cao, X. Jin, Q. N. Zhang, *J. Theor. Comput. Chem.* **2005**, *4*, 593–602.
[50] M. F. Perutz, A. J. Wilkinson, M. Paoli, G. G. Dodson, *Annu. Rev. Biophys. Biomol. Struct.* **1998**, *27*, 1–34.
[51] M. C. Durrant, *Biochem. J.* **2001**, *355*, 569–576.
[52] R. K. Szilagyi, D. G. Musaev, K. Morokuma, *Theochem* **2000**, *506*, 131–146.
[53] I. Dance, *Biochemistry* **2006**, *45*, 6328–6340.
[54] D. J. Lowe, K. Fisher, R. N. F. Thorneley, *Biochem. J.* **1990**, *272*, 621–625.
[55] J. Kästner, P. E. Blöchl, *J. Am. Chem. Soc.* **2007**, *129*, 2998–3006.
[56] I. G. Dance, K. J. Fisher, *Prog. Inorg. Chem.* **1994**, *41*, 637–803.
[57] R. J. Deeth, *New Sci.* **1997**, 24–27.
[58] "Brajendra Nath Seal", to be found under http://en.wikipedia.org/wiki/Brajendra_Nath_Seal, **2007**.

Received: April 16, 2007
Published online: July 5, 2007

  